

Synthesis and evaluation of a ^{18}F -labeled 4-phenylpiperidine-4-carbonitrile radioligand for σ_1 receptor imaging

Jiajun Ye,^a Xia Wang,^a Winnie Deuther-Conrad,^b Jinming Zhang,^c Jianzhou Li,^a Xiaojun Zhang,^c Liang Wang,^a Jörg Steinbach,^b Peter Brust^b and Hongmei Jia^{a*}

We report the design and synthesis of several 4-phenylpiperidine-4-carbonitrile derivatives as σ_1 receptor ligands. *In vitro* radioligand competition binding assays showed that all the ligands exhibited low nanomolar affinity for σ_1 receptors ($K_i(\sigma_1) = 1.22\text{--}2.14\text{ nM}$) and extremely high subtype selectivity ($K_i(\sigma_2) = 830\text{--}1710\text{ nM}$; $K_i(\sigma_2)/K_i(\sigma_1) = 680\text{--}887$). [^{18}F]9 was prepared in 42–46% isolated radiochemical yield, with a radiochemical purity of >99% by HPLC analysis after purification, via nucleophilic $^{18}\text{F}^-$ substitution of the corresponding tosylate precursor. Biodistribution studies in mice demonstrated high initial brain uptakes and high brain-to-blood ratios. Administration of SA4503 or haloperidol 5 min prior to injection of [^{18}F]9 significantly reduced the accumulation of radiotracers in organs known to contain σ_1 receptors. Two radioactive metabolites were observed in the brain at 30 min after radiotracer injection. [^{18}F]9 may serve as a lead compound to develop suitable radiotracers for σ_1 receptor imaging with positron emission tomography.

Keywords: fluorine-18; σ_1 receptor; positron emission tomography; 4-phenylpiperidine-4-carbonitrile derivatives; molecular probe

Introduction

Sigma-1 (σ_1) receptor has been identified as a unique ligand-operated molecular chaperone recently.¹ This protein consists of 223 amino acids with a 25 kDa molecular mass and possesses two trans-membrane domains.^{2,3} It serves as a modulator of inter-organelle communications and regulates a variety of cellular function.^{4–6} Increasing evidence has shown that σ_1 receptors play an important role in neuronal plasticity and are associated with various neuropsychiatric diseases.^{4–8} Moreover, they are involved in cardiovascular disease⁹ and human tumors.^{10–12} Development of ligands and molecular imaging agents with high affinity and selectivity for σ_1 receptors will help improve our ability to track, monitor, and understand σ_1 receptor-related diseases.

In the past decades, many radionuclide-labeled ligands such as ^{11}C , ^{18}F , or ^{76}Br -labeled σ_1 receptor positron emission tomography (PET) imaging agents and $^{99\text{m}}\text{Tc}$, ^{123}I -labeled single-photon emission computed tomography (SPECT) imaging agents have been reported.¹³ Among them, only a few ligands such as [^{11}C]SA4503,^{14–16} [^{18}F]FPS,¹⁷ and [^{123}I]TPCNE¹⁸ (Figure 1) have been evaluated in humans. Moreover, [^{18}F]FPS¹⁹ and [^{123}I]TPCNE¹⁸ have shown irreversible kinetics in human studies. For the first useful radiotracer [^{11}C]SA4503, its use in clinic needs an on-site cyclotron. More recently, [^{18}F]fluspidine^{20,21} and [^{18}F]FTC-146^{22,23} (Figure 1) have proved to be promising PET radiotracers for visualizing σ_1 receptors. However, further investigation is still required for their clinical translation. Therefore, there is a need for the development of ^{18}F -labeled radiotracers with appropriate affinity and high specificity for σ_1 receptors.

It was reported that 1-benzyl-4-phenylpiperidine-4-carbonitrile (compound 1) showed subnanomolar affinity for σ_1 receptors

and 1600-fold subtype selectivity as well as no affinity for opioid receptors.²⁴ Thus, compound 1 appears to be an ideal lead compound to design radionuclide-labeled probes to investigate σ_1 receptor function. In this paper, we replaced the hydrogen atom at the *para*-position of the *N*-benzyl moiety of compound 1 with F, I, or $\text{OCH}_2\text{CH}_2\text{F}$ group for assessment of maintained affinity and selectivity (Figure 2). Moreover, we synthesized a ^{18}F -labeled radiotracer and evaluated its potential as a PET probe for imaging σ_1 receptor through biodistribution and blocking studies in mice and radiometabolite studies.

Results and discussion

Chemistry

The synthetic routes of 4-phenylpiperidine-4-carbonitrile derivatives are illustrated in Scheme 1. 4-Hydroxybenzaldehyde reacted with 1-bromo-2-fluoroethane, followed by reduction with NaBH_4 and

^aKey Laboratory of Radiopharmaceuticals (Beijing Normal University), Ministry of Education, College of Chemistry, Beijing Normal University, Beijing 100875, China

^bHelmholtz-Zentrum Dresden-Rossendorf, Department of Neuroradiopharmaceuticals, Institute of Radiopharmaceutical Cancer Research, 04318 Leipzig, Germany

^cNuclear Medicine Department, Chinese PLA General Hospital, Beijing 100853, China

*Correspondence to: Hongmei Jia, Key Laboratory of Radiopharmaceuticals (Beijing Normal University), Ministry of Education, College of Chemistry, Beijing Normal University, Beijing 100875, China.

E-mail: hmjia@bnu.edu.cn

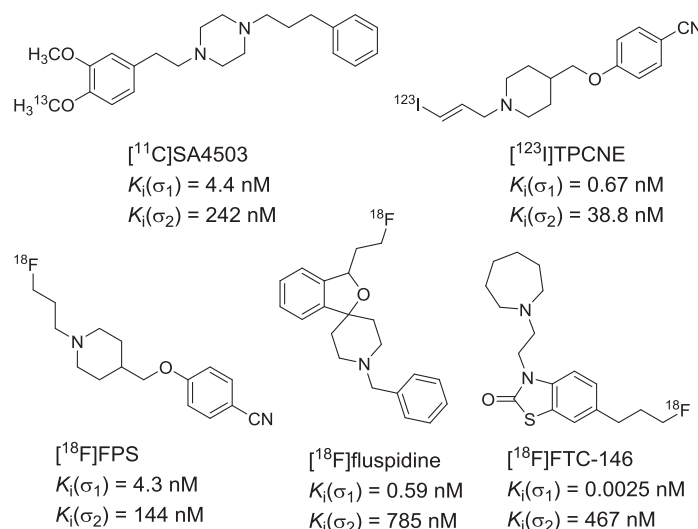


Figure 1. Potent σ_1 receptor radiotracers developed recently.

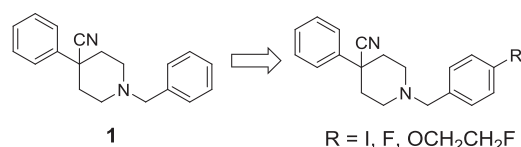
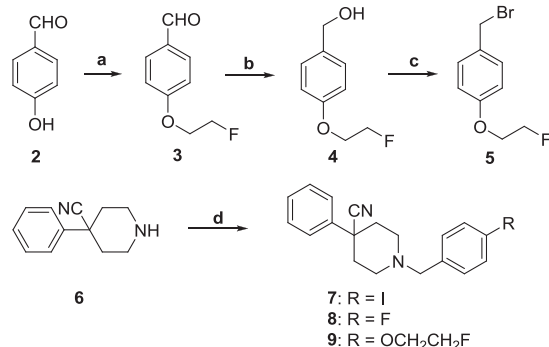


Figure 2. Design concept of 4-phenylpiperidine-4-carbonitrile derivatives.



Scheme 1. Synthetic routes of 4-phenylpiperidine-4-carbonitrile derivatives. Regents and conditions: (a) 1-bromo-2-fluoroethane, K₂CO₃, dimethylformamide, 100 °C, 99%; (b) ethanol, NaBH₄, 85%; (c) CH₂Cl₂, PBr₃, 0 °C, 93%; (d) for **7**, 4-iodobenzyl bromide, acetonitrile, K₂CO₃, KI, 90 °C, 95%; for **8**, 4-fluorobenzyl bromide, acetonitrile, K₂CO₃, KI, 90 °C, 75%; for **9**, 5, CH₂Cl₂, NaH, r.t., 62%.

bromination to obtain intermediate **5**. Compared with the reported method in the literature,^{25,26} the synthetic method of compound **5** in this paper can avoid use of toxic carbon tetrachloride. Moreover, this method has the advantages of high yields and easy separation between the reactants and the products. *N*-Alkylation of compound **6** with 4-iodobenzyl bromide, 4-fluorobenzyl bromide, or intermediate **5** under basic conditions provided target compounds **7**, **8**, and **9**, respectively.

The target compounds (**7**, **8**, and **9**) were analyzed by high-performance liquid chromatography (HPLC) with purity of more than 95%. They were characterized by ¹H NMR, ¹³C NMR, and high-resolution mass spectrometry.

In vitro radioligand competition studies

The competition binding assays for σ_1 and σ_2 receptors of 4-phenylpiperidine-4-carbonitrile derivatives were performed as previously reported.²⁷ The binding assays used rat brain with (+)-[³H]pentazocine as radioligand for the σ_1 receptors and rat liver membranes with [³H]DTG (in the presence of 10 μ M dextralorphan) as radioligand for the σ_2 receptors. The results are shown in Table 1. Replacement of hydrogen atom in the phenyl group with I, F, or OCH₂CH₂F at the para-position of compound **1** slightly decreased the affinity for σ_1 receptors (compounds **7**, **8**, and **9** vs. compound **1**). However, they still possessed low nanomolar affinity for σ_1 receptors (1.22–2.14 nM) and high subtype selectivity (680–887 fold).

For compounds **7–9**, calculated log *P* (clog *P*) values obtained by the CHEMDRAW software are 4.52, 3.54, and 3.57, respectively. It is well-known that lipophilicity is a critical physicochemical parameter for a radiotracer, as it impacts upon its ability to cross the blood–brain barrier (BBB), the free fraction in the plasma and in the brain, as well as non-specific binding.^{28,29} Considering the relatively lower lipophilicity of compound **9** with fluoroethoxy moiety compared with compound **7** with I atom, and the simpler radiolabeling method compared with that required for compound **8**, the corresponding radioligand [¹⁸F]**9** was prepared

Table 1. Binding affinities of the 4-phenylpiperidine-4-carbonitrile derivatives for σ_1 receptors and σ_2 receptors^a

Compound	$K_i(\sigma_1)$ (nM)	$K_i(\sigma_2)$ (nM)	$K_i(\sigma_2)/K_i(\sigma_1)$
1 ^b	0.41 ± 0.08	657 ± 19	1602
7	2.14 ± 0.38	1710 ± 650	799
8	1.22 ± 0.44	830 ± 370	680
9	1.47 ± 0.89	1304 ± 475	887
Haloperidol ^c	4.95 ± 1.74	20.7 ± 0.07	4

^aValues are means ± standard deviation (SD) of at least two experiments performed in triplicate.

^bFrom reference.²⁴

^cFrom reference.²⁶

and evaluated for its potential as a σ_1 receptor radiotracer for PET imaging.

Radiolabeling

The synthesis of the precursor and [^{18}F]**9** is depicted in Scheme 2. Reductive amination of compound **6** with 4-hydroxybenzaldehyde in the presence of $\text{NaBH}(\text{OAc})_3$ led to intermediate **10**, which reacted with ethylene glycol bistosylate to give the tosylate precursor **11** in 71% yield. The radioligand [^{18}F]**9** is obtained through a direct $\text{S}_{\text{N}}2$ displacement of the tosylate group in precursor **11** with [^{18}F]fluoride (in the formation of kryptofix $2.2.2/\text{K}^+/[^{18}\text{F}]^-$ complex). After removing inorganic salts via a Waters C18 plus Sep-Pak cartridge, the crude product was purified by an isocratic semi-preparative radio-HPLC using a reverse-phase column and a mobile phase consisting of acetonitrile and water (containing 10 mM NH_4OAc) (65:35, v/v) at a flow rate of 4 mL/min. The radioactive peak corresponding to [^{18}F]**9** was collected, diluted with water, and passed across a C18 Sep-Pak cartridge. The product was eluted off with ethanol and diluted with sterile saline to provide a solution with approximately 300 kBq of radioactivity per 0.1 mL.

In order to identify the radiotracer, [^{18}F]**9** and the corresponding unlabeled compound **9** were co-injected and co-eluted. Their HPLC profiles using acetonitrile and water (containing 10 mM NH_4OAc) (65/35, v/v) as mobile phase at a flow rate of 1 mL/min are presented in Figure 3. The retention times of unlabeled compound **9** and [^{18}F]**9** were 12.77 and 12.83 min, respectively. The difference in retention time was corresponding to the time lag as a result of the volume and flow rate within the distance between the UV and radioactivity detectors of our HPLC system. After purification by semi-preparative radio-HPLC, the radiochemical purity (RCP) of [^{18}F]**9** was >99%. The overall isolated radiochemical yield was 42–46% ($n=3$, corrected for decay). The total synthesis time was approximately 1 h. The specific activity of [^{18}F]**9** was 23.56 GBq/ μmol .

The *in vitro* stability of [^{18}F]**9** in saline was evaluated by measuring the RCP at different time points. After 1, 2, and 3 h, the RCPs of [^{18}F]**9** were still >99%, indicating high stability of [^{18}F]**9** *in vitro* (Figure 4).

A shake-flask method was employed for the determination of lipophilicity of the radiotracer in terms of the apparent distribution coefficient in a 1-octanol and 0.05 mol/L potassium phosphate buffer system at pH 7.4 as previously reported.^{26,30} The log *D* value of [^{18}F]**9** was 3.29 ± 0.15 ($n=3$), which is within the range expected to have good BBB permeability.

Biodistribution and blocking studies in male ICR mice

In order to evaluate the kinetics of [^{18}F]**9**, biodistribution studies were performed in male ICR mice. The results are summarized in

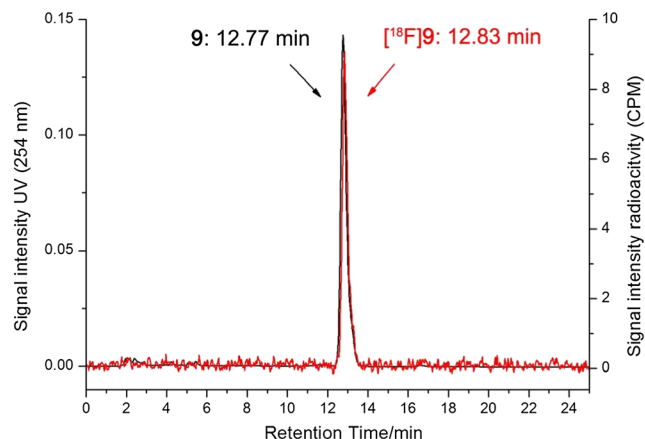
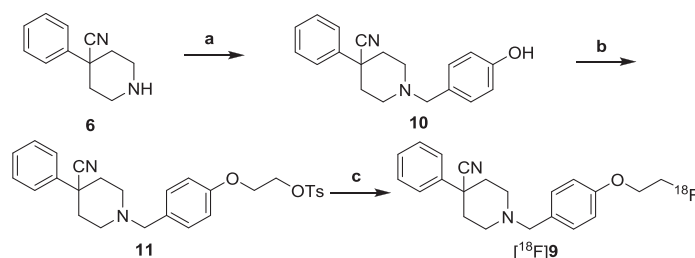


Figure 3. High-performance liquid chromatography (HPLC) co-elution profile of **9** and [^{18}F]**9**, $t_{\text{R}} = 12.77$ min, [^{18}F]**9** $t_{\text{R}} = 12.83$ min (65% acetonitrile and 35% water containing 10 mM NH_4OAc , 1 mL/min).

Table 2. [^{18}F]**9** exhibited high initial brain uptake with $11.10 \pm 1.28\%$ ID/g at 2 min after radiotracer injection. The accumulation in the brain was highest at 2 min after radiotracer injection and slowly decreased thereafter with $9.32 \pm 0.92\%$ ID/g at 15 min, $7.49 \pm 1.01\%$ ID/g at 30 min, $4.84 \pm 1.17\%$ ID/g at 60 min, and $3.30 \pm 0.22\%$ ID/g at 120 min. The radiotracer levels in the blood were relatively low with $1.03 \pm 0.08\%$ ID/g at 2 min, $1.01 \pm 0.15\%$ ID/g at 15 min, and $1.47 \pm 0.23\%$ ID/g at 30 min, resulting in high brain-to-blood ratios of 10.8, 9.2, and 5.1 at 2, 15, and 30 min, respectively. The accumulation in the blood was increased with time, especially at 30 min after radiotracer injection. [^{18}F]**9** also showed relatively fast washout in the organs known to contain σ_1 receptors, including the lungs, kidneys, heart, spleen, and liver. Finally, the accumulation of radiotracer in the bone is almost the same within 30 min and increased slightly thereafter with $6.37 \pm 0.90\%$ ID/g at 120 min, indicating that [^{18}F]**9** may undergo defluorination *in vivo*.

In order to verify the specific binding of [^{18}F]**9** to σ_1 receptors *in vivo*, the effects of preadministration of haloperidol (0.1 mL, 1 mg/kg) and SA4503 (3 $\mu\text{mol/kg}$) on the biodistribution of radiotracer in various organs of male ICR mice were investigated. The blocking agent was injected 5 min prior to the radiotracer injection (0.1 mL, about 300 kBq). Blocking results of organ distribution of [^{18}F]**9** at 15 and 30 min after radiotracer injection in ICR mice are summarized in Figure 5. Pretreatment of animals with haloperidol and SA4503 resulted in significant reduction of radiotracer uptake in organs known to contain σ_1 receptors at 15 min, including the brain (65–66%, $p < 0.001$), heart (35–37%, $p < 0.001$), liver (36–51%, $p < 0.001$), spleen (56–58%, $p < 0.001$), kidney (45–49%, $p < 0.001$), and lungs (44–49%, $p < 0.01$). The



Scheme 2. Synthesis of the precursor and [^{18}F]**9**. Reagents and conditions: (a) 4-hydroxybenzaldehyde, 1,2-dichloroethane, $\text{NaBH}(\text{OAc})_3$, 72%; (b) ethylene glycol bistosylate, acetonitrile, K_2CO_3 , 90 °C, 71%; (c) [^{18}F]F $^-$, acetonitrile, Kryptofix 2.2.2, K_2CO_3 , 90 °C, 7 min.

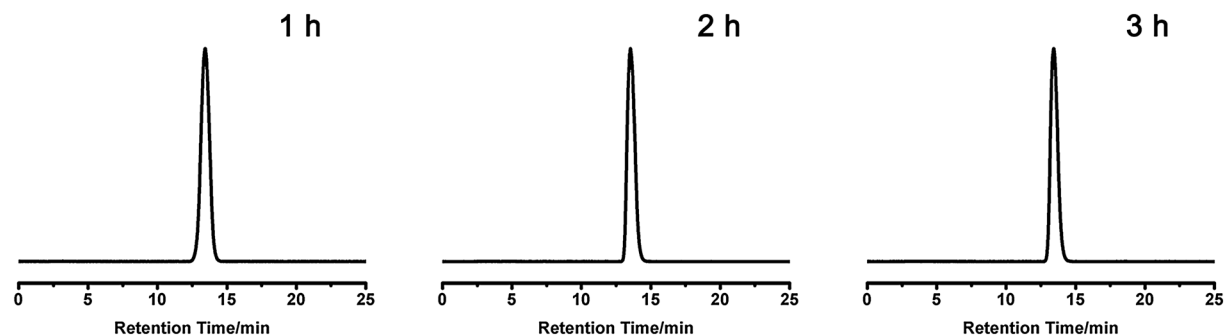


Figure 4. Analytical radio-HPLC chromatograms of the *in vitro* stability of [^{18}F]9 in saline at 1, 2, and 3 h (65% acetonitrile and 35% water containing 10 mM NH_4OAc , 1 mL/min).

Table 2. Biodistribution of [^{18}F]9 in male ICR mice^a

Organ	2 min	15 min	30 min	60 min	120 min
Blood	1.03 ± 0.08	1.01 ± 0.15	1.47 ± 0.23	2.35 ± 0.20	2.73 ± 0.27
Brain	11.10 ± 1.28	9.32 ± 0.92	7.49 ± 1.01	4.84 ± 1.17	3.30 ± 0.22
Heart	19.11 ± 2.52	5.76 ± 0.31	3.90 ± 0.41	3.28 ± 0.45	3.11 ± 0.34
Liver	5.17 ± 1.46	8.14 ± 0.76	7.74 ± 1.02	6.17 ± 1.02	4.00 ± 0.33
Spleen	3.46 ± 1.66	7.47 ± 1.14	7.29 ± 0.95	4.88 ± 0.69	3.74 ± 0.70
Lung	41.14 ± 12.32	8.56 ± 1.09	6.18 ± 1.24	4.42 ± 0.70	3.46 ± 0.27
Kidney	18.15 ± 3.25	9.57 ± 0.93	6.84 ± 0.36	4.59 ± 0.62	3.23 ± 0.41
Small intestine ^b	5.62 ± 1.37	7.17 ± 1.48	5.11 ± 0.86	7.08 ± 1.31	8.56 ± 1.62
Stomach ^b	1.54 ± 0.14	1.86 ± 0.53	1.55 ± 0.21	1.96 ± 0.69	1.26 ± 0.13
Muscle	4.36 ± 0.81	2.98 ± 0.15	2.54 ± 0.14	2.53 ± 0.30	2.64 ± 0.32
Bone (femur)	3.04 ± 0.54	2.89 ± 0.52	2.79 ± 0.74	3.95 ± 0.46	6.37 ± 0.90
Brain/Blood	10.8	9.2	5.1	2.1	1.2
Brain/Bone	3.7	3.2	2.7	1.2	0.5

^aData are expressed as percentage of injected dose per gram, means ± SD, $n = 5$.

^bPercentage of injected dose per organ.

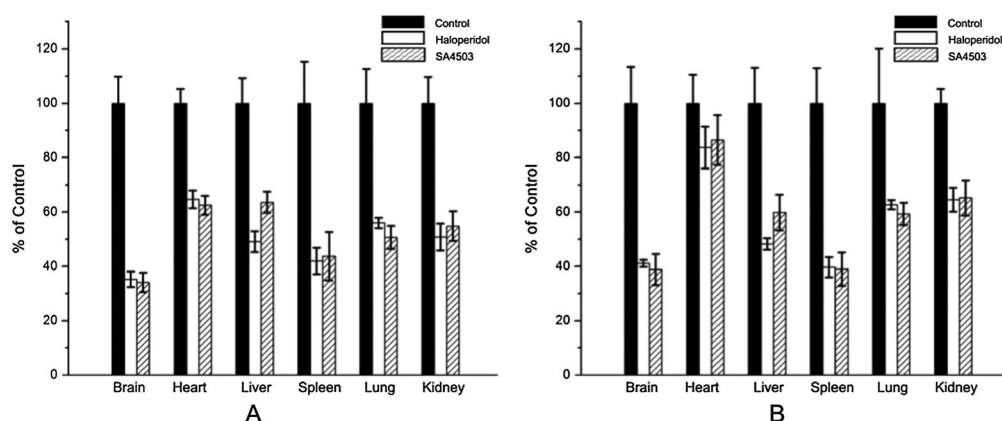


Figure 5. Effects of pretreatment with haloperidol (0.1 mL, 1 mg/kg, 2.7 $\mu\text{mol/kg}$) or SA4503 (0.1 mL, 3 $\mu\text{mol/kg}$) 5 min prior to the injection of radiotracer [^{18}F]9 (0.1 mL, about 300 kBq) at 15 min (A) and 30 min (B) after intravenous administration. Multiple tests including Student's *t*-test (independent, two-tailed) and one-way ANOVA with a post-hoc test were performed, and $p < 0.05$ (except for SA4503 in the heart at 30 min). Values are means ± SD, $n = 5$.

blocking rate at 30 min was slightly less than that at 15 min, including the brain (59–61%, $p < 0.001$), heart (14–16%, $p < 0.05$ except for SA4503), liver (40–52%, $p < 0.001$), spleen (60–61%, $p < 0.001$), kidney (35%, $p < 0.001$), and lungs (37–41%, $p < 0.01$). These data demonstrated that [^{18}F]9 binds to σ_1 receptors specifically *in vivo*.

In vivo metabolic stability of [^{18}F]9

It is well known that the metabolism profile of the radiotracer *in vivo* is a very important issue for brain imaging. The metabolic profile of [^{18}F]9 was investigated in plasma and brain samples obtained from mice at 30 min after radiotracer injection as

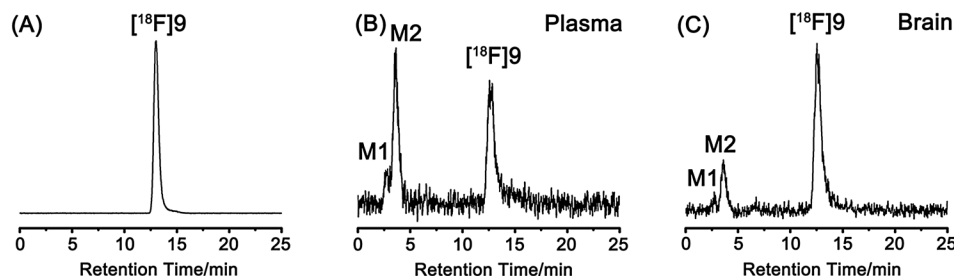


Figure 6. Analytical radio-HPLC chromatograms of the plasma and brain samples at 30 min after administration of [^{18}F]9 in mice.

previously reported.³⁰ Protein precipitation was performed by using ice-cold acetonitrile. Acetonitrile extracts were analyzed and quantified by radio-HPLC. Representative HPLC chromatograms are given in Figure 6.

At 30 min after radiotracer injection, 47% of the total radioactivity was represented by the parent radiotracer [^{18}F]9 with the retention time of 12.8 min in plasma samples. Two hydrophilic radioactive metabolites M1 (9%) and M2 (44%) were observed with retention times of 3.0 and 3.6 min, respectively. In the brain samples, 74% of the total radioactivity was represented by [^{18}F]9. Similar to what was found in plasma, two hydrophilic radioactive metabolites M1 (5%) and M2 (21%) were observed with retention times of 3.0 and 3.6 min, respectively.

Currently, more and more studies have proved that the σ_1 receptors are linked to various human brain diseases. Neuroimaging of σ_1 receptors with optimal radiotracers provides an important tool to investigate the σ_1 receptors in the pathophysiology of neuropsychiatric diseases. The decreased density of σ_1 receptors was observed using [^{11}C]SA4503 imaging studies in patients with Parkinson's disease¹⁵ and Alzheimer's disease.¹⁴ However, [^{11}C]SA4503 needs an on-site cyclotron which limited its applications in clinic. Among the potential σ_1 receptor radiotracers up to date, [^{18}F]FPS and [^{123}I]TPCNE were not optimal as a result of their irreversible kinetics in humans. [^{18}F]fluspidine and [^{18}F]FTC-146 are still waiting for human studies. In this study, compounds **7**, **8**, and **9** exhibited low nanomolar affinity for σ_1 receptors and extremely high subtype selectivity. Considering higher detection sensitivity and resolution of imaging with PET than that with SPECT and simple synthesis of ^{18}F -labeled radiotracers via nucleophilic $^{18}\text{F}^-$ substitution of the corresponding tosylate precursor, [^{18}F]9 was synthesized and evaluated for its potential as σ_1 receptor radiotracer. High *in vitro* stability of [^{18}F]9 in saline was observed. The lipophilicity of [^{18}F]9 ($\log D_{\text{pH } 7.4} = 3.29$) is appropriate for BBB penetration. Compared with [^{11}C]SA4503³¹ and [^{18}F]fluspidine,²⁰ [^{18}F]9 showed higher initial brain uptake, higher brain-to-blood ratios within 15 min, and lower brain-to-blood ratios thereafter. Consistent with defluorination *in vivo*, [^{18}F]9 exhibited higher brain-to-bone ratios within 30 min and lower brain-to-bone ratios thereafter. Pretreatment of animals with haloperidol and SA4503 resulted in significant reduction of radiotracer uptake in organs known to contain σ_1 receptors at 15 and 30 min, indicating specific binding of [^{18}F]9 *in vivo*. Moreover, this radiotracer exhibited comparable specific binding to σ_1 receptors in the brain to [^{11}C]SA4503³¹ and [^{18}F]fluspidine.²⁰ Compared with [^{18}F]fluspidine (98%),²⁰ the percentage of parent radiotracer [^{18}F]9 in the brain (74%) at 30 min after radiotracer injection was lower, suggesting that the stability of [^{18}F]9 in the brain is apparently poorer than [^{18}F]fluspidine. Different with [^{18}F]fluspidine,²⁰ two radioactive metabolites M1 and M2, which could be attributed to radiofluoride

($t_R = 3.0$ min) and another compound ($t_R = 3.6$ min), were observed in the brain and blood, indicating that radioactive metabolites may cross the BBB. To investigate the effects of radioactive metabolites on the accuracy of the brain PET signal, identification of the radioactive metabolites and measurement of their affinities for σ_1 receptors need to be performed. We will use such information to refine the structure of [^{18}F]9 for improved metabolic stability in the future.

Conclusion

We have synthesized three 4-phenylpiperidine-4-carbonitrile derivatives with high affinity for σ_1 receptors and very high subtype selectivity. [^{18}F]9 has been obtained in good radiochemical yield and high radiochemical purity. The $\log D$ value of [^{18}F]9 was within the range expected to show excellent brain uptake. In biodistribution studies in mice, [^{18}F]9 displayed high initial brain uptake and high brain-to-blood ratios. Blocking studies confirmed high specific binding of [^{18}F]9 to σ_1 receptors *in vivo*. Identification of two radioactive metabolites in the brain is useful to refine the structure of [^{18}F]9 for improved metabolic stability. [^{18}F]9 may serve as a lead compound to develop suitable PET radiotracers for σ_1 receptor imaging. Radiolabeled **7** and **8** would be of future interests.

Experimental section

General method

All reagents and chemicals were obtained from commercial suppliers and used without further purification unless otherwise stated. Thin-layer chromatography (silica gel 60 F₂₅₄ plates Merck) was used to monitor the reactions. Flash column chromatography was carried out on silica gel (200–400 mesh) using the mobile phase indicated in the experimental procedure. Melting points (Mps) were measured using a WRX-4 micro melting point apparatus (Shanghai Yice Apparatus & Equipment Co., LTD, China) and were uncorrected. ^1H and ^{13}C NMR spectra were recorded on a Bruker Avance III NMR spectrometer at 400 MHz (^1H) and 100 MHz (^{13}C). Chemical shifts (δ) are reported in ppm downfield from tetramethylsilane and coupling constants (J) in Hertz (Hz). Mass spectra were acquired by Quattro micro API ESI/MS (Waters, USA). High-resolution mass spectrometry was performed on a LCT Premier XE ESI-TOF mass spectrometry instrument (Waters, USA).

The semi-preparative radio-HPLC was equipped with an Alltech 626 pump and UVSI 200 detector. Samples were separated on an Agela Venusil MP C18 column (250 \times 10 mm, 5 μm) using 65% acetonitrile and 35% water (containing 10 mM NH_4OAc) as mobile phase at a flow rate of 4 mL/min. HPLC analyses were performed on a Shimadzu SCL-20 AVP HPLC system (Shimadzu Corporation, Japan) equipped with a SPD-M20A UV-VIS detector operating at a wavelength of 254 nm and a Bioscan Flow Count 3200 NaI/PMT-radiation scintillation detector. The

samples were analyzed on an Agela Venusil MP C18 column (250 × 4.6 mm, 5 μm) using 65% acetonitrile and 35% water (containing 10 mM NH₄OAc) as mobile phase at a flow rate of 1 mL/min.

Male ICR mice (22–24 g, 4–5 weeks) were purchased from Beijing Vital river experimental animal technical Co., LTD. All procedures of the animal experiments were performed in compliance with relevant laws and institutional guidelines. All of the animal experiments were approved by the Institutional Animal Care and Use Committee of Beijing Normal University.

4-(2-Fluoroethoxy)benzaldehyde (3)

A mixture of 4-hydroxybenzaldehyde (2, 1.01 g, 8.28 mmol), 1-bromo-2-fluoroethane (2.05 g, 16.1 mmol), and K₂CO₃ (2.49 g, 18.0 mmol) in dimethylformamide (20 mL) was stirred at 100 °C for 5 h. The mixture was concentrated under vacuum, and the residue was dissolved in CH₂Cl₂, washed with water, dried with MgSO₄, and concentrated under vacuum to provide **3** as a yellow solid (1.37 g, 99%). Mp: 49.5–51.1 °C. ¹H NMR (400 MHz, CDCl₃) δ (ppm): 9.90 (s, 1H), 7.86 (d, *J* = 8.7 Hz, 2H), 7.04 (d, *J* = 8.6 Hz, 2H), 4.80 (dt, *J* = 47.3, 4.0 Hz, 2H), 4.31 (dt, *J* = 27.5, 4.1 Hz, 2H). ESI-MS, [M + H]⁺: *m/z* = 169.1.

(4-(2-Fluoroethoxy)phenyl)methanol (4)

To a solution of compound **3** (1.45 g, 8.63 mmol) in ethanol (20 mL), NaBH₄ (0.813 g, 21.4 mmol) was added. The mixture was stirred at room temperature for 15 min. Then the reaction was quenched with water, neutralized with dilute hydrochloric acid, and extracted with CH₂Cl₂. The combined organic layer was dried with MgSO₄ and concentrated under vacuum. The residue was purified by column chromatography (silica gel, petroleum ether/ethyl acetate = 10: 1, v/v) to provide **4** as a white solid (1.24 g, 85%). Mp: 45.3–48.8 °C. ¹H NMR (400 MHz, CDCl₃) δ (ppm): 7.31 (d, *J* = 8.5 Hz, 2H), 6.92 (d, *J* = 4.3 Hz, 2H), 4.76 (dt, *J* = 47.3, 4.1 Hz, 2H), 4.63 (s, 2H), 4.22 (dt, *J* = 27.7, 4.1 Hz, 2H).

1-(2-Fluoroethoxy)-4-(bromomethyl)benzene (5)

To a solution of compound **4** (0.206 g, 1.21 mmol) in anhydrous CH₂Cl₂ (10 mL) at 0 °C, PBr₃ (0.475 g, 1.75 mmol) was added. The mixture was stirred at 0 °C for 3 h and then quenched with saturated NaHCO₃ and extracted with CH₂Cl₂. The combined organic layer was dried with MgSO₄ and concentrated under vacuum to provide **5** as a colorless oil (0.262 g, 93%). ¹H NMR (400 MHz, CDCl₃) δ (ppm): 7.33 (d, *J* = 8.6 Hz, 2H), 6.89 (d, *J* = 8.6 Hz, 2H), 4.76 (dt, *J* = 47.4, 4.1 Hz, 2H), 4.50 (s, 2H), 4.21 (dt, *J* = 27.8, 4.1 Hz, 2H).

1-(4-Iodobenzyl)-4-phenylpiperidine-4-carbonitrile (7)

A mixture of 4-phenylpiperidine-4-carbonitrile (**6**, 0.391 g, 2.10 mmol), 4-iodobenzyl bromide (0.624 g, 2.10 mmol), K₂CO₃ (2.89 g, 20.9 mmol), and KI (0.265 g, 1.60 mmol) in acetonitrile (100 mL) was stirred at 90 °C for 60 min. The mixture was concentrated under vacuum. The residue was dissolved in CH₂Cl₂, washed with saturated NaCl, dried with MgSO₄, concentrated under vacuum and purified by column chromatography (silica gel, petroleum ether/ethyl acetate = 4: 1, v/v) to provide **7** as a white solid (0.804 g, 95%). Mp: 105.3–105.5 °C. ¹H NMR (400 MHz, CDCl₃) δ (ppm): 7.67 (d, *J* = 8.0 Hz, 2H), 7.51 (d, *J* = 7.6 Hz, 2H), 7.41 (t, *J* = 7.5 Hz, 2H), 7.34 (t, *J* = 7.2 Hz, 1H), 7.11 (d, *J* = 7.9 Hz, 2H), 3.55 (s, 2H), 2.99 (d, *J* = 11.9 Hz, 2H), 2.58–2.46 (m, 2H), 2.17–2.08 (m, 4H). ¹³C NMR (101 MHz, CDCl₃) δ (ppm): 140.24, 137.67, 131.28, 129.26, 128.37, 125.82, 122.16, 93.04, 62.31, 50.86, 42.80, 36.62. HRMS (ESI-ToF), [M + H]⁺: *m/z* calcd for C₁₉H₂₀IN₂ 403.0666, found 403.0672.

1-(4-Fluorobenzyl)-4-phenylpiperidine-4-carbonitrile (8)

Compound **6** (0.298 g, 1.60 mmol) and 4-fluorobenzyl bromide (0.397 g, 2.10 mmol) were dissolved in anhydrous acetonitrile (100 mL), followed by addition of K₂CO₃ (2.17 g, 15.7 mmol) and KI (0.199 g, 1.20 mmol).

The mixture was stirred at 90 °C for 60 min. The mixture was concentrated under vacuum, and the residue was dissolved in CH₂Cl₂, washed with saturated NaCl, dried with MgSO₄, and concentrated under vacuum. The residue was purified by column chromatography (silica gel, petroleum ether/ethyl acetate = 4: 1, v/v) to provide **8** as a white solid (0.353 g, 75%). Mp: 82.0–82.5 °C. ¹H NMR (400 MHz, CDCl₃) δ (ppm): 7.54–7.49 (m, 2H), 7.45–7.38 (m, 2H), 7.38–7.30 (m, 3H), 7.08–6.98 (m, 2H), 3.58 (s, 2H), 2.99 (d, *J* = 12.2 Hz, 2H), 2.60–2.48 (m, 2H), 2.15–2.06 (m, 4H). ¹³C NMR (101 MHz, CDCl₃) δ (ppm): 162.24 (d, *J*_{C-F} = 243.5 Hz), 140.44, 134.10 (d, *J*_{C-F} = 3.1 Hz), 130.71 (d, *J*_{C-F} = 7.9 Hz), 129.20, 128.28, 125.81, 122.25, 115.32 (d, *J*_{C-F} = 21.1 Hz), 62.22, 50.81, 42.92, 36.75. HRMS (ESI-ToF), [M + H]⁺: *m/z* calcd for C₁₉H₂₀FN₂ 295.1605, found 295.1615.

1-(4-(2-Fluoroethoxy)benzyl)-4-phenylpiperidine-4-carbonitrile (9)

Compounds **5** (0.103 g, 0.442 mmol) and **6** (0.0815 g, 0.438 mmol) were dissolved in anhydrous CH₂Cl₂ (10 mL), followed by addition of NaH (0.0180 g, 0.750 mmol). The mixture was stirred at room temperature for 24 h. Then the reaction was quenched with water, extracted with ethyl acetate. The combined organic layer was dried with MgSO₄, concentrated under vacuum, and purified by column chromatography (silica gel, petroleum ether/ethyl acetate/triethylamine = 20: 1: 1, v/v/v) to provide **9** as a colorless solid (0.0929 g, 62%). Mp: 58.6–60.0 °C. ¹H NMR (400 MHz, CDCl₃) δ (ppm): 7.53–7.25 (m, 7H), 6.90 (d, *J* = 8.6 Hz, 2H), 4.76 (ddd, *J* = 47.4, 5.4, 4.2 Hz, 2H), 4.22 (ddd, *J* = 27.8, 4.2, 3.0 Hz, 2H), 3.55 (s, 2H), 2.99 (d, *J* = 12.2 Hz, 2H), 2.55–2.43 (m, 2H), 2.10 (s, 4H). ¹³C NMR (100 MHz, CDCl₃) δ (ppm): 157.74, 140.30, 130.76, 130.33, 128.98, 128.04, 125.63, 122.11, 114.52, 81.92 (d, *J*_{C-F} = 169.7 Hz), 67.20 (d, *J*_{C-F} = 10.3 Hz), 62.24, 50.61, 42.82, 36.58. ESI-MS, [M + H]⁺: *m/z* = 339.3. HRMS (ESI-ToF), [M + H]⁺: *m/z* calcd for C₂₁H₂₄FN₂O 339.1873, found 339.1874.

1-(4-Hydroxybenzyl)-4-phenylpiperidine-4-carbonitrile (10)

To a solution of compound **6** (0.192 g, 1.03 mmol) in 1,2-dichloroethane (5 mL), 4-hydroxybenzaldehyde (0.257 g, 2.10 mmol), and NaBH(OAc)₃ (0.609 g, 2.87 mmol) were added. The mixture was stirred at room temperature for 24 h. Then the reaction was quenched with saturated NaHCO₃, extracted with CH₂Cl₂. The combined organic layer was dried with MgSO₄ and concentrated under vacuum. The residue was purified by column chromatography (silica gel, petroleum ether/ethyl acetate/triethylamine = 4: 1, v/v) to provide **10** as a white solid (0.218 g, 72%). Mp: 104.7–107.2 °C. ¹H NMR (400 MHz, CDCl₃) δ (ppm): 7.49 (d, *J* = 7.7 Hz, 2H), 7.39 (t, *J* = 7.2 Hz, 2H), 7.32 (t, *J* = 7.3 Hz, 1H), 7.19 (d, *J* = 8.2 Hz, 2H), 6.73 (d, *J* = 8.3 Hz, 2H), 3.57 (s, 2H), 3.06 (d, *J* = 11.7 Hz, 2H), 2.54 (t, *J* = 11.7 Hz, 2H), 2.25–2.00 (m, 4H). ESI-MS, [M + H]⁺: *m/z* = 293.3.

2-(4-((4-Cyano-4-phenylpiperidin-1-yl)methyl)phenoxy)ethyl-4-methylbenzenesulfonate (11)

A mixture of **10** (0.0651 g, 0.223 mmol), ethylene glycol bistosylate (0.187 g, 0.505 mmol), and K₂CO₃ (0.0721 g, 0.522 mmol) in anhydrous acetonitrile (8 mL) was stirred at 90 °C for 24 h. The mixture was concentrated under vacuum, dissolved in CH₂Cl₂, washed with saturated NaCl, dried with MgSO₄, and concentrated under vacuum. The residue was purified by column chromatography (silica gel, petroleum ether/ethyl acetate/triethylamine = 4: 1, v/v) to provide **11** as a white solid (0.0775 g, 71%). Mp: 91.0–92.4 °C. ¹H NMR (400 MHz, CDCl₃) δ (ppm): 7.83 (d, *J* = 8.3 Hz, 2H), 7.44–7.30 (m, 7H), 7.23 (d, *J* = 7.9 Hz, 2H), 6.76 (d, *J* = 8.5 Hz, 2H), 4.36 (dd, *J* = 4.9, 3.4 Hz, 2H), 4.15 (dd, *J* = 4.9, 3.4 Hz, 2H), 3.53 (s, 2H), 2.98 (d, *J* = 11.3 Hz, 2H), 2.54–2.38 (m, 5H), 2.09 (s, 4H). ¹³C NMR (100 MHz, CDCl₃) δ (ppm): 157.31, 144.92, 140.23, 132.95, 130.91, 130.31, 129.85, 128.99, 128.03, 125.63, 122.12, 114.42, 68.12, 65.51, 62.22, 50.60, 42.81, 36.56, 21.66. ESI-MS, [M + H]⁺: *m/z* = 491.9.

Radiochemistry

[^{18}F]fluoride was produced through the nuclear reaction of $^{18}\text{O}(\text{p}, \text{n})^{18}\text{F}$ using proton beam bombardment of the target (20 MeV, 65 μA) for 15 min in a Sumitomo HM-20S cyclotron. Then [^{18}F]fluoride was transported to the QMA column via nitrogen carrier gas and eluted into a reaction vessel using a solution of Kryptofix 2.2.2 (13 mg) and potassium carbonate (1.1 mg) in $\text{CH}_3\text{CN}/\text{H}_2\text{O}$ (0.8 mL/0.2 mL). The solvent was removed at 120 °C under a stream of nitrogen. The residue was dried three times with 1 mL of anhydrous acetonitrile each at 120 °C, followed by addition of a solution of the tosylate precursor **11** (6 mg/mL) in anhydrous acetonitrile (0.6 mL). The mixture was stirred at 90 °C for 7 min to provide [^{18}F]**9**. After being diluted with water and trapped on a Waters C18 plus Sep-Pak cartridge, the product was eluted off the cartridge with anhydrous acetonitrile and loaded onto a sample loop in the isocratic semi-preparative radio-HPLC for purification (Agela Venusil MP C18 column, 250 mm \times 10 mm, 5 μm , eluent 65% CH_3CN and 35% H_2O containing 10 mM NH_4OAc , flow rate 4 mL/min). The product peak was collected, diluted with water, and trapped on a Waters C18 plus Sep-Pak cartridge. The cartridge was washed with water. The product was eluted off the cartridge with ethanol. Radiochemical purity was analyzed by analytical radio-HPLC (Agela Venusil MP C18 column, 250 \times 4.6 mm, 5 μm , eluent 65% CH_3CN , and 35% H_2O containing 10 mM NH_4OAc , flow rate 1 mL/min). For animal experiments, [^{18}F]**9** was formulated as a saline solution containing no more than 7% ethanol.

Determination of log *D* value

The distribution coefficient of [^{18}F]**9** was determined by measuring the distribution of the radiotracer between 1-octanol and potassium phosphate buffer (PBS, 0.05 mol/L, pH 7.4). The radiotracer [^{18}F]**9** (10 μL , 1100 kBq) was mixed with 1-octanol (3 mL) and potassium phosphate buffer (3 mL) in a centrifuge tube (15 mL). The tube was vortexed for 3 min, followed by centrifugation at 3500 rpm for 5 min (AnkeTDL80-2B, China). About 0.05 mL of 1-octanol layer was weighed in a tared tube. About 0.5 mL of the PBS layer was weighed in a second tared tube. After addition of 0.5 mL of buffer to the 1-octanol fraction and 0.05 mL of 1-octanol to the aqueous fraction, activity in both tubes was measured in an automatic gamma-counter (Wallac 1470 Wizard, USA). The log *D* value was calculated as the ratio of the cpm/mL of 1-octanol to that of PBS and expressed as $\log D = \log [\text{cpm/mL}(1\text{-octanol})/\text{cpm/mL}(\text{PBS})]$. The samples from the remaining organic layer were repartitioned until consistent distribution coefficient values were obtained. The measurement was carried out in triplicate and repeated three times.

In vitro stability studies

The *in vitro* stability of [^{18}F]**9** was evaluated by monitoring the radiochemical purity (RCP) at different time points. A saline solution of [^{18}F]**9** was standing at room temperature for up to 3 h. The RCP was determined by radio-HPLC chromatography at 1, 2, and 3 h (Shimadzu system, Agela Venusil MP C18 column, 250 \times 4.6 mm, 5 μm , eluent 65% CH_3CN , and 35% H_2O containing 10 mM NH_4OAc , flow rate 1 mL/min).

In vitro radioligand competition studies

All the procedures for the σ receptor competition studies were previously described.²⁷ The σ_1 receptor assay was carried out with (+)-[^3H]-pentazocine ($K_d = 6.9 \pm 1.1 \text{ nM}$)³² as the radioligand using rat brain membrane homogenates. The σ_2 receptor affinity was performed using rat liver membrane homogenates with the radioligand [^3H]DTG ($K_d = 29.2 \pm 2.8 \text{ nM}$)³³ in the presence of 10 μM dextrallorphan ($K_i(\sigma_1) = 125 \pm 12 \text{ nM}$)³⁴ for selective masking of σ_1 receptor binding sites. Nonspecific binding was determined with addition of 10 μM haloperidol. Apparent binding affinity (K_i) values were calculated according to the Cheng-Prusoff equation and represent data from at least two independent experiments, each performed in triplicate. The results are given as means \pm standard deviation (SD).

Biodistribution and blocking studies in male ICR mice

A saline solution of [^{18}F]**9** (0.1 mL, about 300 kBq) was intravenously injected into mice (five groups, $n = 5$ in each group) via the tail vein. The mice were sacrificed by decapitation at 2, 15, 30, 60, and 120 min after radiotracer injection. Samples of blood, whole brain, heart, liver, spleen, lungs, kidneys, muscle, and bone (femur) were removed, weighed, and counted in an automatic counter (Wallac 1470 Wizard, USA). The percentage of injected dose per gram of wet tissue (% ID/g) was calculated by a comparison of the tissue count to suitably diluted aliquots of the injected radiotracer as counting standards. All radioactivity measurements were corrected for decay. The results are given as means \pm SD.

For the blocking studies, the mice were intravenously injected via the tail vein with haloperidol (0.1 mL, 1 mg/kg, 2.7 $\mu\text{mol/kg}$) or SA4503 (0.1 mL, 3 $\mu\text{mol/kg}$) 5 min prior to the injection of [^{18}F]**9** (0.1 mL, about 300 kBq). The mice were decapitated at 15 or 30 min after radiotracer injection. The blood and organs of interest were isolated and analyzed as described in the preceding texts. Significant differences between control and test groups were determined by multiple tests including Student's *t*-test (independent, two-tailed) and one-way ANOVA with a post-hoc test. The criterion for significance was $p \leq 0.05$. Data given in the figures are means \pm SD.

In vivo metabolic stability of [^{18}F]**9**

The *in vivo* metabolic fate of [^{18}F]**9** was performed in male ICR mice. The mice were intravenously injected with a saline solution of [^{18}F]**9** (0.1 mL, 11.1 MBq) via the tail vein and sacrificed by decapitation at 30 min after injection. The plasma and brain were collected. The brain was washed with saline. The samples were placed separately in 2 mL of ice-cold CH_3CN and homogenized with a homogenizer (LabGEN 7) for 2 min. The mixture was centrifuged at 14000 rpm for 5 min (Eppendorf Centrifuge 5418). The combined supernatants were collected and passed through a 0.22 μm organic Millipore filter. The filtrates were concentrated to 0.1 mL under a stream of nitrogen gas flow and injected into the radio-HPLC for analysis (Shimadzu system, Agela Venusil MP C18 column, 250 \times 4.6 mm, 5 μm , eluent 65% CH_3CN , and 35% H_2O containing 10 mM NH_4OAc , flow rate 1 mL/min).

Acknowledgement

This work was supported by the National Natural Science Foundation of China (no. 21471019).

References

- [1] T. Hayashi, T.-P. Su, *Cell* **2007**, *131*, 596–610.
- [2] M. Hanner, F. F. Moebius, A. Flandorfer, H. G. Knaus, J. Striessnig, E. Kempner, H. Glossmann, *Proc. Natl. Acad. Sci. U. S. A.* **1996**, *93*, 8072–8077.
- [3] E. Aydar, C. P. Palmer, V. A. Klyachko, M. B. Jackson, *Neuron* **2002**, *34*, 399–410.
- [4] T. Maurice, T.-P. Su, *Pharmacol. Ther.* **2009**, *124*, 195–206.
- [5] H. Teruo, T. Shang-Yi, M. Tomohisa, F. Michiko, S. Tsung-Ping, *Expert Opin. Ther. Targets* **2011**, *15*, 557–577.
- [6] S. Kourrich, T.-P. Su, M. Fujimoto, A. Bonci, *Trends Neurosci.* **2012**, *35*, 762–771.
- [7] J. A. Fishback, M. J. Robson, Y.-T. Xu, R. R. Matsumoto, *Pharmacol. Ther.* **2010**, *127*, 271–282.
- [8] L. Nguyen, B. P. Lucke-Wold, S. A. Mookerjee, J. Z. Cavendish, M. J. Robson, A. L. Scandinaro, R. R. Matsumoto, *Jpn. J. Pharmacol.* **2015**, *127*, 17–29.
- [9] K. Ito, Y. Hirooka, R. Matsukawa, M. Nakano, K. Sunagawa, *Cardiovasc. Res.* **2011**, *93*, 33–40.
- [10] A. van Waarde, A. A. Rybczynska, N. K. Ramakrishnan, K. Ishiwata, P. H. Elsinga, R. A. J. O. Dierckx, *Curr. Pharm. Des.* **2010**, *16*, 3519–3537.
- [11] M. Happy, J. Dejoie, C. K. Zajac, B. Cortez, K. Chakraborty, J. Aderemi, M. Sauane, *Biochem. Biophys. Res. Commun.* **2015**, *456*, 683–688.

- [12] A. van Waarde, A. A. Rybczynska, N. K. Ramakrishnan, K. Ishiwata, P. H. Elsinga, R. A. J. O. Dierckx, *Biochim. Biophys. Acta, Biomembrs* **2015**, 1848, 2703–2714.
- [13] P. Brust, W. Deuther-Conrad, K. Lehmkuhl, H. Jia, B. Wünsch, *Curr. Med. Chem.* **2014**, 21, 35–69.
- [14] M. Mishina, M. Ohyama, K. Ishii, S. Kitamura, Y. Kimura, K.-i. Oda, K. Kawamura, T. Sasaki, S. Kobayashi, Y. Katayama, K. Ishiwata, *Ann. Nucl. Med.* **2008**, 22, 151–156.
- [15] M. Mishina, K. Ishiwata, K. Ishii, S. Kitamura, Y. Kimura, K. Kawamura, K. Oda, T. Sasaki, O. Sakayori, M. Hamamoto, S. Kobayashi, Y. Katayama, *Acta Neurol. Scand.* **2005**, 112, 103–107.
- [16] J. Toyohara, M. Sakata, K. Ishiwata, *Cent. Nerv. Syst. Agents Med. Chem.* **2009**, 9, 190–196.
- [17] R. N. Waterhouse, M. S. Nobler, Y. Zhou, R. C. Chang, O. Morales, H. Kuwabawa, A. Kumar, R. L. VanHeertum, D. F. Wong, H. A. Sackeim, *Neuroimage* **2004**, 22, T29–T30.
- [18] J. M. Stone, E. Årstad, K. Erlandsson, R. N. Waterhouse, P. J. Ell, L. S. Pilowsky, *Synapse* **2006**, 60, 109–117.
- [19] R. N. Waterhouse, R. C. Chang, N. Atuehene, T. L. Collier, *Synapse* **2007**, 61, 540–546.
- [20] S. Fischer, C. Wiese, E. Große Maestrup, A. Hiller, W. Deuther-Conrad, M. Scheunemann, D. Schepmann, J. Steinbach, B. Wünsch, P. Brust, *Eur. J. Nucl. Med. Mol. Imaging* **2011**, 38, 540–551.
- [21] P. Brust, W. Deuther-Conrad, G. Becker, M. Patt, C. K. Donat, S. Stittsworth, S. Fischer, A. Hiller, B. Wenzel, S. Dukic-Stefanovic, S. Hesse, J. Steinbach, B. Wünsch, S. Z. Lever, O. Sabri, *J. Nucl. Med.* **2014**, 55, 1730–1736.
- [22] M. L. James, B. Shen, C. L. Zavaleta, C. H. Nielsen, C. Mesangeau, P. K. Vuppala, C. Chan, B. A. Avery, J. A. Fishback, R. R. Matsumoto, S. S. Gambhir, C. R. McCurdy, F. T. Chin, *J. Med. Chem.* **2012**, 55, 8272–8282.
- [23] M. L. James, B. Shen, C. H. Nielsen, D. Behera, C. L. Buckmaster, C. Mesangeau, C. Zavaleta, P. K. Vuppala, S. Jamalapuram, B. A. Avery, D. M. Lyons, C. R. McCurdy, S. Biswal, S. S. Gambhir, F. T. Chin, *J. Nucl. Med.* **2014**, 55, 147–153.
- [24] S. L. Mercer, J. Shaikh, J. R. Traynor, R. R. Matsumoto, A. Coop, *Eur. J. Med. Chem.* **2008**, 43, 1304–1308.
- [25] K. Kopka, A. Faust, P. Keul, S. Wagner, H.-J. Breyholz, C. Holtke, O. Schober, M. I. Schafers, B. Levkau, *J. Med. Chem.* **2006**, 49, 6704–6715.
- [26] X. Wang, Y. Li, W. Deuther-Conrad, F. Xie, X. Chen, M.-C. Cui, X.-J. Zhang, J.-M. Zhang, J. Steinbach, P. Brust, B.-L. Liu, H.-M. Jia, *Bioorg. Med. Chem.* **2013**, 21, 215–222.
- [27] C. Fan, H. Jia, W. Deuther-Conrad, P. Brust, J. Steinbach, B. Liu, *Sci. China, Ser. B: Chem* **2006**, 49, 169–176.
- [28] M. Laruelle, M. Slifstein, Y. Huang, *Mol. Imaging Biol.* **2003**, 5, 363–375.
- [29] Y. Huang, M.-Q. Zheng, J. M. Gerdes, *Curr. Top. Med. Chem.* **2010**, 10, 1499–1526.
- [30] Y. Li, X. Wang, J. Zhang, W. Deuther-Conrad, F. Xie, X. Zhang, J. Liu, J. Qiao, M. Cui, J. Steinbach, P. Brust, B. Liu, H. Jia, *J. Med. Chem.* **2013**, 56, 3478–3491.
- [31] K. Kawamura, K. Ishiwata, Y. Shimada, Y. Kimura, T. Kobayashi, K. Matsuno, Y. Homma, M. Senda, *Ann. Nucl. Med.* **2000**, 14, 285–292.
- [32] K. Matsuno, M. Nakazawa, K. Okamoto, Y. Kawashima, S. Mita, *Eur. J. Pharmacol.* **1996**, 306, 271–279.
- [33] T. Senda, K. Matsuno, S. Mita, *Neurosci. Res. Commun.* **1995**, 17, 97–105.
- [34] B. J. Vilner, W. D. Bowen, *J. Pharmacol. Exp. Ther.* **2000**, 292, 900–911.